LANGMUIR Article
Cite This: Langmuir 2019, 35, 9677−9683
pubs.acs.org/Langmuir

Atmospheric Pressure Plasma Deposition of Hydrophilic/Phobic Patterns and Thin Film Laminates on Any Surface

A. Demaude,*[,†] C. Poleunis,[‡] E. Goormaghtigh,[§] P. Viville,[∥] R. Lazzaroni,[∥] A. Delcorte,[‡] M. Gordon,[⊥] and F. Reniers[†]

[†]Faculty of Sciences, Chemistry of Surfaces, Interfaces and Nanomaterials - ChemSIN, Université libre de Bruxelles, cp 255, Avenue F.D. Roosevelt 50, B-1050 Bruxelles, Belgium

[‡]Institute of Condensed Matter and Nanosciences, Université Catholique de Louvain, Place Louis Pasteur 1, Box L4.04.10, B-1348 Louvain-la-Neuve, Belgium

[§]Structure and Function of Biological Membranes, Center for Structural Biology and Bioinformatics, Université libre de Bruxelles, Boulevard du Triomphe, CP 206/2, B-1050 Brussels, Belgium

[∥]Laboratory for Chemistry of Novel Materials, Université de Mons, Place du Parc 20, 7000 Mons, Belgium

[⊥]Department of Chemical Engineering, University of California−Santa Barbara, Eng II #3351, Santa Barbara, California 93106-5080, United States

ABSTRACT: Patterned and layered hydrophilic/phobic coatings were deposited on multiple surfaces using nonfluorinated precursors (AA, acrylic acid; PMA, propargyl methacrylate) with an atmospheric pressure dielectric barrier discharge operating in open air. Water contact angles of the resulting films could be tuned from <5° (superhydrophilic) to >135° (very hydrophobic) by adjusting the AA/PMA feed ratio and/or via postdeposition exposure of films to an Ar/O_2 plasma treatment. Coatings could be applied to any surface and were seen to be water stable, due in large part to cross-linking induced from the reactivity of the PMA pendant groups. Hybrid hydrophilic/phobic patterns at sub-millimeter length scales, and philic/phobic/philic laminates were produced using a shadow mask and sequential deposition, respectively. Chemical heterogeneity of films was assessed using XPS, SIMS, and micro-IR imaging and suggest that localization of COOH and OH groups are primarily responsible for hydrophilicity. Overall, this work demonstrates that atmospheric pressure plasma polymerization is a simple and scalable method for robust and tunable control of wettability of surfaces of all kinds.

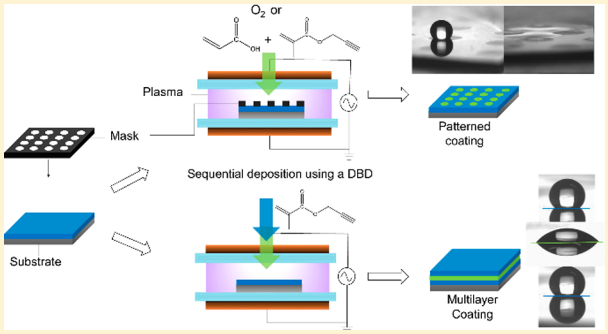

INTRODUCTION

Hybrid surfaces possessing both hydrophilic and hydrophobic functionalities can be found in nature[1,2] and are also being explored for a variety of technological applications such as directing fluid motion in microfluidic devices,[3] controlling cell growth on biomedical surfaces,[4] and to impart antifouling or self-cleaning properties.[5,6] For example, the Stenocara beetle (Figure 1) that lives in desert regions uses patterned hydrophilic "bumps" and hydrophobic "channel" regions to harvest and funnel fog, respectively.[7] Multilayer or laminate coatings with alternating hydrophilic and phobic character have also been used to control cell adhesion[8] and potentially in marine and biological environments to inhibit fouling. Traditional approaches to deposit such coatings utilize a combination of photolithography, chemical vapor deposition, and/or location-specific covalent grafting of perfluorinated or aliphatic species on the surface;[9−11] unfortunately, these methods are often tedious, expensive, not scalable, and/or involve potentially hazardous chemical agents.

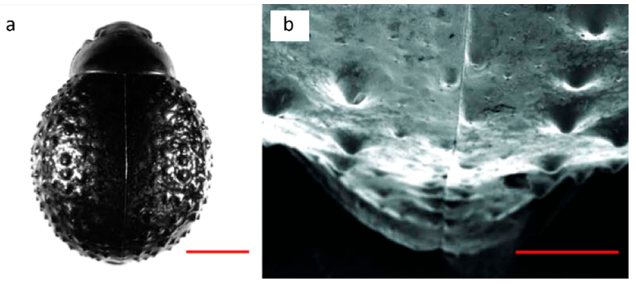

Figure 1. Stenocara beetle (*Physasterna cribripes*) and scanning electron micrograph of the textured surface on its back. Left and right scale bars correspond to 5 mm and 1 mm, respectively. Images are from ref 13.

Received: February 19, 2019
Revised: May 21, 2019
Published: July 9, 2019

DOI: 10.1021/acs.langmuir.9b00493
Langmuir 2019, 35, 9677−9683

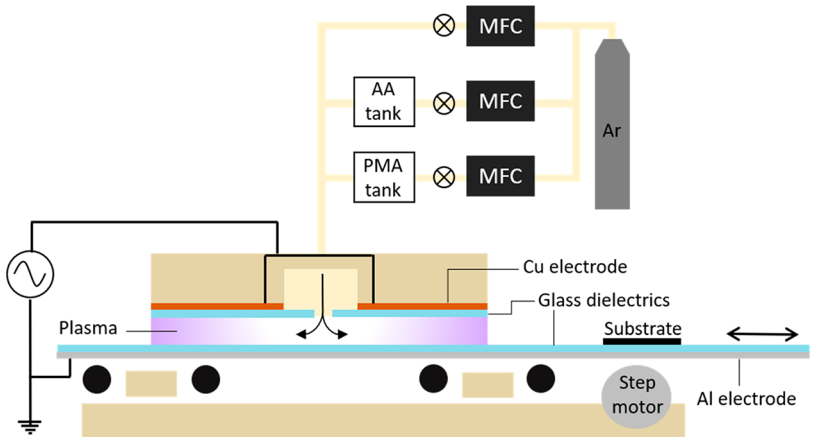

Figure 2. Schematic of the dielectric barrier discharge (DBD) plasma system used to deposit hybrid hydrophilic/phobic films.

Plasmas, on the other hand, have been used to prepare (e.g., clean, make reactive, change adhesion) and modify surfaces to have hydrophilic or hydrophobic character, but infrequently both. One example does exist where a dielectric barrier discharge (DBD) plasma was used to locally graft hydrophilic functionalities to a fluorinated polymer (hydrophobic) substrate using a physical mask.[12] Given the potential utility of these hydrophilic/phobic surfaces in many technological venues, it is important to develop simple and robust techniques to create them, as well as apply them to different materials.

In this work, we demonstrate a simple, scalable, and tunable method, based on atmospheric pressure plasma deposition of polymer-like films, which can produce hydrophilic/phobic patterns and thin film laminates on virtually any surface. Acrylic acid (AA) and propargyl methacrylate (PMA) precursors were fed to an atmospheric pressure DBD running in Ar to create hydrophilic and/or phobic films. As-deposited PMA coatings were very hydrophobic (WCA > 125°), but they could be easily rendered hydrophilic (WCA < 5°) with a simple O_2-plasma treatment. Alternatively, AA (which can be of interest for biocompatibility) can be codeposited with PMA to tune the WCA from philic to phobic, which, via cross-linking facilitated with PMA,[14,15] results in hybrid films that are exceptionally water stable, contrary to most pure AA films. Moreover, to our knowledge, synthesis of philic/phobic laminates by atmospheric pressure plasmas has not been reported; this approach, and the resulting coatings, may find application in antifouling situations[8] and for water filtration membranes.[16]

Stable hydrophilic/phobic 2D patterns in the hundreds of micrometers to millimeter length scale regime were created using sequential deposition through a PVC mask, and water contact angle (WCA) contrast of 25° and 125°, respectively, could be obtained. Hydrophilic/phobic laminates of ∼300 nm thick were created by stepwise deposition with a DBD plasma "curtain" for film deposition rates of ∼1 nm/s.

X-ray photoelectron spectroscopy (XPS), microinfrared analysis (μ-IR), and time-of-flight secondary ion mass spectrometry (TOF-SIMS) showed that hydrophilic regions (e.g., patterns or laminates) were enriched in carboxylic acid moieties and had higher $C{=}O/CH_2CH_3$ ratios.

EXPERIMENTAL SECTION

The atmospheric pressure DBD plasma system used in this work is schematically shown in Figure 2 and summarized in detail elsewhere.[17] The discharge was operated at 16.2 kHz (30, 60, and 90 W). The total argon flow was kept at 20 L/min with 1 to 3 L/min diverted through glass bubblers (25 °C) containing the acrylic acid (AA) and propargyl methacrylate (PMA) (98%) precursors (purchased from Sigma-Aldrich and Alpha Aesar, and used as received).

The DBD had glass plate dielectrics with the gas feed entered through a slit in the upper (powered) electrode. The substrate was positioned on a rolling stage controlled via stepper motor. Gas feeds to the plasma and presursor cells were controlled by mass flow controllers (MFCs). Prior to each deposition, the reactor was thoroughly cleaned using methanol and acetone, and the substrate (Si wafer or Al plate) was first "activated" in a pure argon plasma at 60 W for 150 s (i.e., one pass of the substrate through the DBD). Thin films were then deposited by entraining precursors in the Ar feed to the DBD (1−3 L/min to bubblers, with total Ar flow = 20 L/min) with two and four substrate "passes" (150 s exposure/pass) through the discharge for Si and Al substrates, respectively. When both precursors were used simultaneously, the gas flow to the DBD was allowed to mix for one pass before striking the plasma. Deposited films were also sometimes treated using an Ar/O_2 plasma (18L/min Ar, 0.1 L/min O_2) at 60 W for one pass. Hydrophilic/phobic patterns were synthesized by plasma deposition through a 140 μm thick microperforated PVC sheet (1 mm holes, from Easyflyer) applied directly on the substrate.

Water contact angles (WCA) of the plasma deposited coatings were determined using a Krüss DSA100 goniometer (static mode) and Drop Shape Analysis software. (Non)-patterned coatings were characterized by deposition of a (3) 0.3 μL droplet of deionized water at 400 μL/min dispensing rate, and all measurements were repeated at least 5 times. Thickness of the deposited films were measured using a DektakXT profilometer. Atomic Force Microscopy (AFM) was used to analyze the surface morphology of plasma deposited films and multilayer samples. AFM images were recorded in air with a Nanoscope IIIa microscope from Bruker operating in tapping mode. The probes were silicon tips with a spring constant of 24−52 N/m, a resonance frequency lying in the 264−339 kHz range and a typical radius of curvature in the 5−10 nm range. The images presented here are recorded with a sampling resolution of 512 × 512 data points and scan sizes of 10 × 10 μm^2.

Infrared reflection absorption spectroscopy (IRRAS, 650−4000 cm^{-1}) and IR imaging (900−3600 cm^{-1}) of the hydrophilic/phobic films were performed using a Nicolet 5700 FTIR spectrometer and Cary 620 FTIR microscope equipped with LN2-cooled HgCdTe detectors, respectively. The analysis area for IR imaging was 2640 × 2640 μm^2 with 128 × 128 pixels and 64 scans/pixel.

X-ray photoelectron spectroscopy (XPS) analysis was performed with a PHI 5600 Physical Electronics photoelectron spectrometer using Mg anode (200 W) with pass energies of 190 and 24 eV for survey and high-resolution scans, respectively. Average surface

DOI: 10.1021/acs.langmuir.9b00493
Langmuir 2019, 35, 9677−9683

concentrations were determined using CasaXPS software with C 1s and O 1s sensitivity factors of 0.205 and 0.63, respectively. The C 1s spectral envelope was fit with a standard Gaussian−Lorentzian, and a Shirley background using the same software. Secondary ion mass spectrometry (SIMS, 200 × 200 μm^2 analysis area) was carried out with a TOF-SIMS5 from IONTOF (Münster, Germany) equipped with a Bi^{5+} ion source (55 fA at 30 keV); samples were sputter cleaned (Ar^+, 3 keV, 5 nA) before SIMS analysis.

RESULTS AND DISCUSSION

Hydrophobic Surfaces. Hydrophobic films were deposited from PMA using different Ar flows to the precursor bubbler (1−3 L/min) and plasma powers (30, 60, 90 W), as detailed in Figure 3. In all cases, films showed hydrophobic

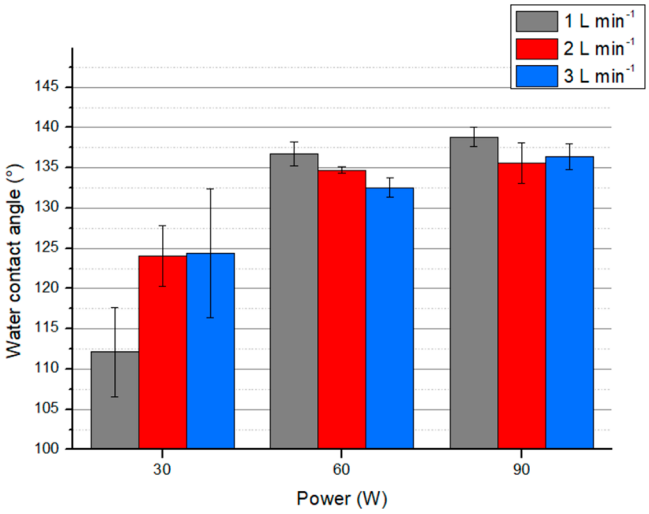

Figure 3. Water contact angles for hydrophobic films produced from the PMA precursor using an atmospheric pressure DBD discharge. Substrate was a Si wafer and Ar gas flow to the PMA bubbler is noted.

character (WCA > 90°), and when deposition conditions were optimized (1−2 L/min, 60 W), superhydrophobic films with WCA > 135° were obtained. In general, WCA increases with plasma power because more energy is given to the system, leading to fragmentation and the loss of polar functional groups, which, in turn, result in more cross-linking and polymerization. Surface roughness, which is known to influence wettability, also contributes to the high WCA observed on the films deposited at 60 and 90 W (>120°, the maximum value that can be found on a flat surface). Indeed, AFM performed on the 60 W film revealed an RMS roughness of 125 ± 5 nm. In addition, we have found that films produced from precursors containing reactive chemical moieties, e.g., alkenes or alkynes, tend to be powdery at high precursor flows.[18] These findings are in good agreement with the surface morphology of PMA coatings studied by SEM in a previous paper,[17] where rough surfaces made up of 50−100 nm globular-like features were observed.

Hydrophilic Surfaces. Hydrophilic films were produced using two methods: (i) postdeposition treatment of the aforementioned hydrophobic PMA films with an Ar/O_2 plasma, and (ii) via direct deposition using mixed PMA and AA precursors. In the former case, O_2 plasma-treated PMA films had WCAs in the 5−25° range, which we believe is due to grafting of polar, oxygen-containing chemical species to the surface (Figure 4b). In the latter case, which may be additionally useful for biocompatibility applications,[14] WCAs were ∼50°. These higher values are likely due to surface COOH moieties provided by the AA precursor (Figure 4b).

Our choice to combine PMA and AA precursors is based on the observation that films deposited from pure AA are often soluble in water,[15,16] and our prior work[17] demonstrating that PMA-like precursors with pendant reactive groups may more easily facilitate cross-linking, and hence stability, of the film. To explore this potentially beneficial effect in more detail, WCAs of films with various PMA/AA precursor ratios were tested before and after immersion in water for 1 h (Figure 4a). In general, water stability of the films increased with the amount of PMA in the precursor mix and with applied power, both of which likely increase cross-linking in the film. However, these two parameters also increase the water contact angle of the film. The best compromise between high hydrophilicity (51°) and good water stability was obtained with a 50/50 Ar flow ratio to PMA/AA at 60 W, which is equivalent to a PMA mass fraction of ∼0.32.

It is interesting to note that O_2-plasma treatment of the PMA film results in superhydrophilicity (WCA < 5°), but after water immersion, the WCA increase to ∼20°. This evolution could be explained by fragmentation of polymeric chains at the film surface, generated by the Ar/O_2 plasma treatment, along with the grafting of polar moieties. When the same is immersed in water, these independent polymeric fragments could be eliminated. Multiple (and short, 20 s) immersion tests confirm this hypothesis, namely a single 20 s rinse is sufficient to see the WCA jump from <5° to 20°, and thereafter, longer and repeated water immersions do not further increase the WCA above ∼20°. Immersion in water of this Ar/O_2 plasma treated coating and the subsequent removal of fragments also leads to a decrease of roughness (RMS of 128.4 nm before rinsing compared to 66.3 nm after rinsing). At unchanged surface composition, this explains also the increase in contact angle. More generally, the change in wettability between the PMA, the Mix, and the AA films can be directly correlated to the introduction of COOH moieties coming from the AA, as shown by the comparison of O−C═O versus C−C component intensities ratio ($I_{O-C=O}/I_{C-C}$) in Figure 4c. From this figure, it also comes up that the decrease in WCA between the PMA and the PMA+O_2 films is not influenced as much by the change in the $I_{O-C=O}/I_{C-C}$ ratio, as the oxygen plasma treatment does not generate specific carboxylic groups at the surface. Indeed, this would rather be explained by the grafting of alcohol moieties, as will be shown later in this paper by comparing the IR spectra of a PMA area and of a O_2-plasma treated PMA area of a hybrid coating (see Figure 9b). This grafting of alcohol moieties at the surface leads to a global increase of the total oxygen surface concentration. This concurs with the comparison of the XPS O 1s versus C 1s peak intensity ratio ($I_{O\ 1s}/I_{C\ 1s}$) with the WCA of the different coatings in Figure 4d, that shows a higher $I_{O\ 1s}/I_{C\ 1s}$ ratio for the PMA+O_2 film compared to the PMA films.

Hydrophilic/Phobic Laminates. Multilayer, hydrophilic/phobic coatings were obtained by alternately depositing PMA and PMA/AA (Mix) films for a total of three layers, i.e., in PMA-Mix-PMA and Mix-PMA-Mix configurations. The wettability of each layer was measured after every plasma deposition step and compared with PMA and Mix-only films, as shown in Figure 5. The data show that the contact angle values of the different films are preserved, even when a film is deposited directly on a surface of the opposite wetting nature. We also note that films deposited on a PMA layer (the second

DOI: 10.1021/acs.langmuir.9b00493
Langmuir 2019, 35, 9677−9683

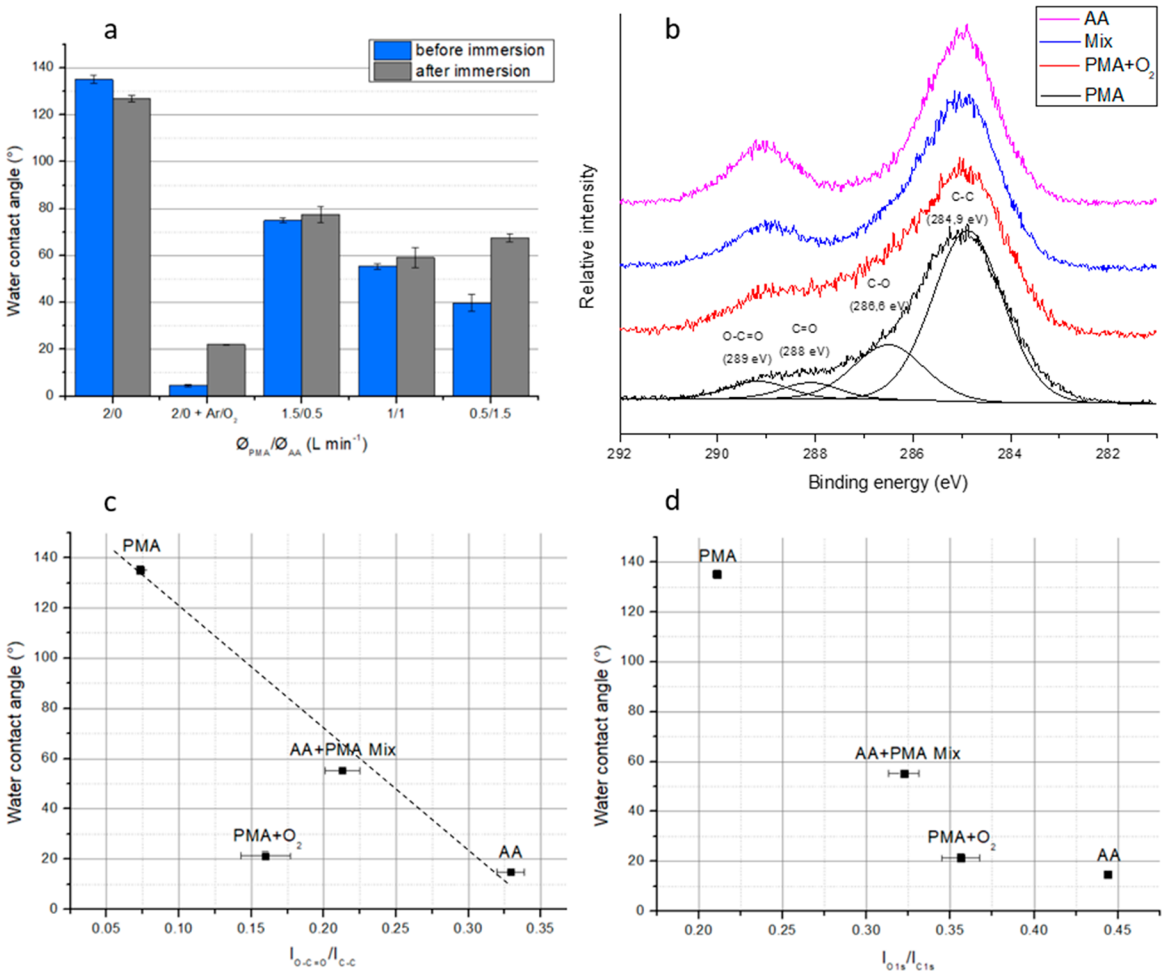

Figure 4. (a) Comparison of WCAs measured on PMA, O_2-plasma treated PMA, and PMA/AA precursor deposited films, before and after immersion in water for 1 h. $Ø_{PMA}/Ø_{AA}$ is the ratio of PMA versus AA in the precursor gas flows, and Ar/O_2 represents the O_2-plasma treatment. Plasma power was 60 W for all samples. (b) XPS of the C 1s spectral envelope of the PMA, O_2-treated PMA ($PMA+O_2$), PMA/AA (Mix) at 1/1 ratio, and pure AA precursor films using 60 W and precursor gas flows of 2 L/min. All envelopes are normalized to the C−C component. Evolution of WCA with the ratio of (c) O−C═O versus C−C component relative intensities obtained from the C 1s high resolution spectra, and (d) O 1s versus C 1s relative intensities for the PMA, $PMA+O_2$, Mix, and AA films obtained from the survey spectra.

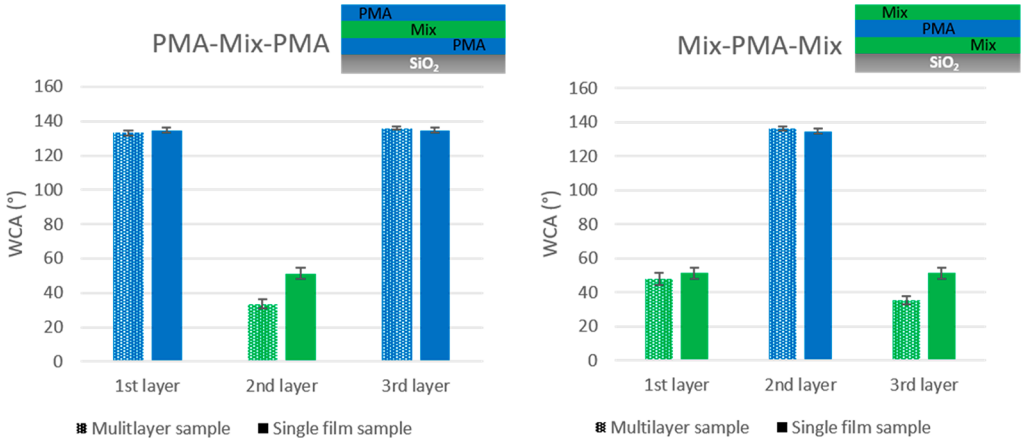

Figure 5. Comparison of WCAs for consecutive layers of hydrophilic/phobic laminate films. Laminates were deposited in two configurations, PMA-Mix-PMA and Mix-PMA-Mix configurations, and compared to their single film counterparts.

layer of PMA-Mix-PMA sample and the third layer of Mix-PMA-Mix sample) show amplified wettability properties (lower WCA) compared to when they were directly deposited on the substrate.

This observation can be explained by comparing the roughness of Mix films directly deposited on the silicon substrate versus deposited on the first PMA layer, of initial roughness of 125 nm. As shown in Figure 6, Mix films

DOI: 10.1021/acs.langmuir.9b00493
Langmuir 2019, 35, 9677−9683

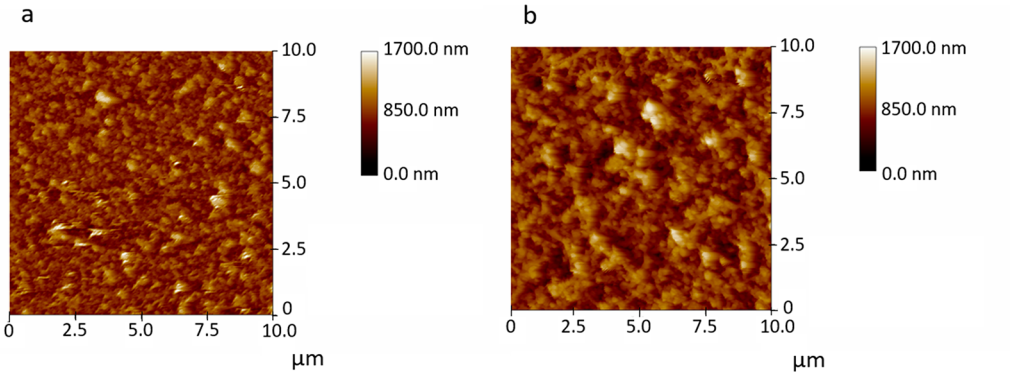

Figure 6. AFM images of (a) a Mix film (RMS = 149 ± 10 nm) deposited on a silicon substrate, and (b) a Mix film (RMS = 187 ± 10 nm) deposited on the first PMA layer.

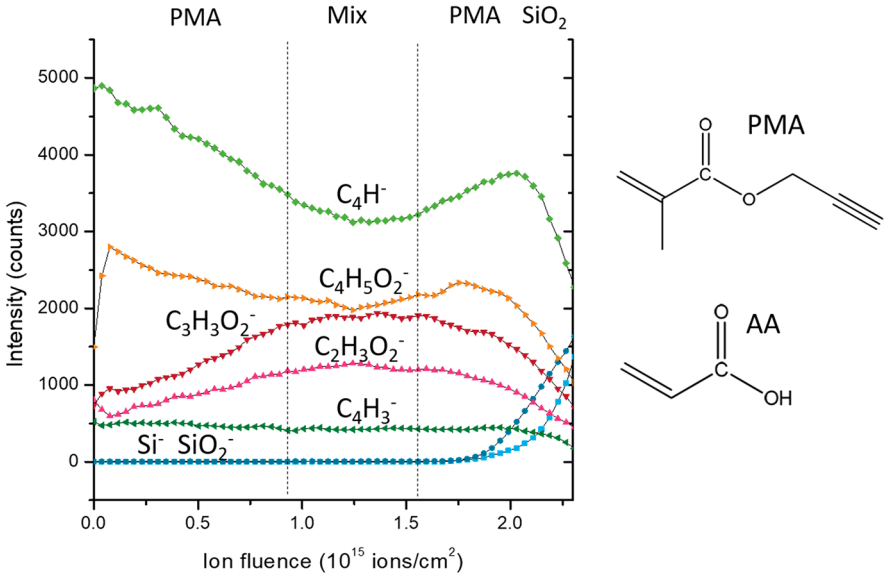

Figure 7. Relative intensity profiles of anions detected in the dynamic SIMS depth profiling analysis of the PMA-Mix-PMA laminate sample.

deposited onto a PMA layer exhibit higher roughness (187 nm versus 149 for Mix films deposited on Si), which leads to a lower contact angle.

The alternating chemistry of these multilayer coatings was examined more closely using SIMS, as depicted in Figure 7 for the PMA-Mix-PMA film. The C_4H^-, $C_4H_3^-$, and $C_4H_5O_2^-$ fragments were selected as indicators of the presence of PMA. Indeed, the signal intensity ratio of C_4H^- compared to $C_4H_3^-$ could highlight cross-linking because it basically consists of replacing a C−H bond by a C−C bond.[19,20] As PMA molecules have one more reactive moiety (alkyne function) compared to AA molecules, they can potentially induce greater cross-linking in the plasma deposited films. Similarly, considering the chemical structure of AA and PMA, the $C_4H_5O_2^-$ ion is more likely to be a fragment of PMA than AA. The relative ion profiles thus confirm that the PMA content is higher in the first and third layers, in good agreement with the deposition sequence. Although the $C_3H_3O_2^-$ (acrylate) and $C_2H_3O_2^-$ (derived from acrylate) ion fragments could be associated with both AA and PMA, the chemical structure of these two precursors suggests that the sputtering of AA will statistically produce a larger relative quantity of these ions than for PMA. Indeed, it is necessary to break more bonds in PMA than AA to generate the $C_3H_3O_2^-$ and $C_2H_3O_2^-$ ions. Moreover, $C_3H_3O_2^-$ is often used as a signature fragment in SIMS analysis of poly(acrylic acid) coatings.[21] The signal intensity of these ions in the depth profile is effectively lower when the intensities of C_4H^- and $C_4H_5O_2^-$ are higher and vice versa, confirming the presence of AA mainly in the middle layer.

Hybrid Hydrophilic/Phobic Patterned Coatings. To demonstrate the utility and ease of direct plasma deposition of patterned hydrophilic/phobic coatings, (hydrophilic) Mix patterns were deposited on (hydrophobic) PMA, and vice versa, namely (hydrophobic) PMA deposited on (hydrophilic) O_2-plasma treated PMA, using a PVC shadow mask (1 mm diameter circles in a hexagonal pattern). Wettability contrast of these surfaces was studied by manually depositing small (0.3 μL) water droplets on the surface in various locations, as shown in Figure 8. Indeed, the hybrid hydrophilic/phobic nature of these surfaces can clearly be seen, particularly for the case of PMA on O_2-treated PMA.

Although water microdroplet measurements on these hybrid patterned films demonstrate their wettability contrast, the local chemistry of various hydrophilic/phobic domains was further investigated using micro-IR imaging. For example, Figure 9 shows how the intensity of the C═O stretching band (~1720−1740 cm^{-1}) varies across the hydrophilic/phobic

DOI: 10.1021/acs.langmuir.9b00493
Langmuir 2019, 35, 9677−9683

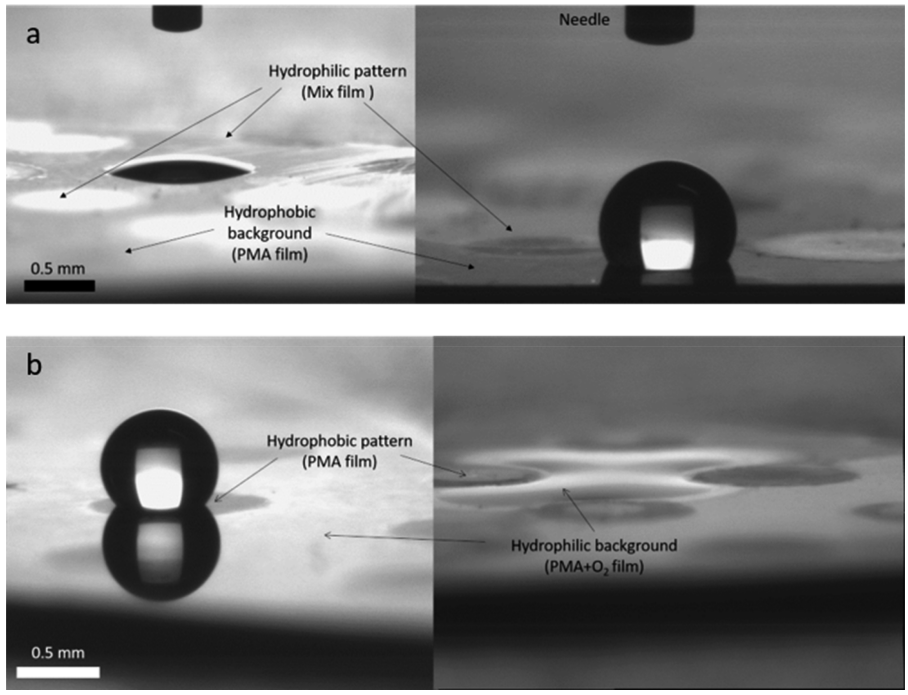

Figure 8. Images of ~0.3 μL water droplets on hybrid patterned hydrophilic/phobic surfaces. (a) Mix on PMA and (b) PMA on O_2-plasma treated PMA.

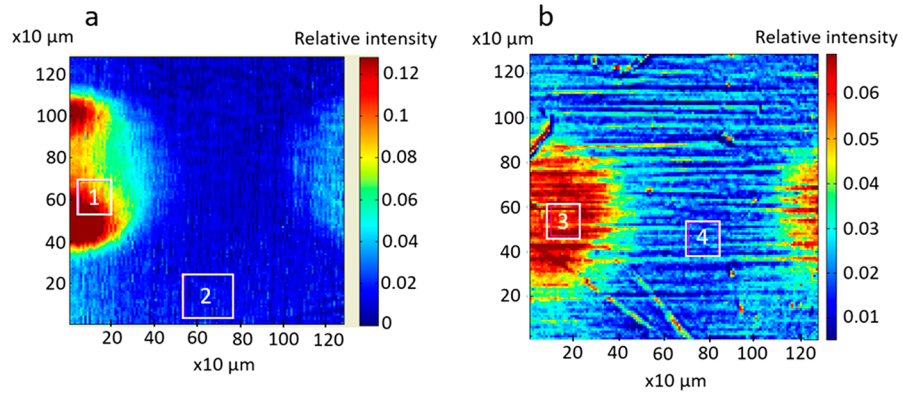

Figure 9. Micro-IR imaging of C═O stretch intensity for hybrid patterned hydrophilic/phobic films. (a) Mix on PMA (1722 cm^{-1}) and (b) PMA on O_2-plasma treated PMA (1734 cm^{-1}). Spectra from regions 1 and 2 in panel a, and spectra from regions 3 and 4 in panel b are shown in Figure 10a and Figure 10b, respectively.

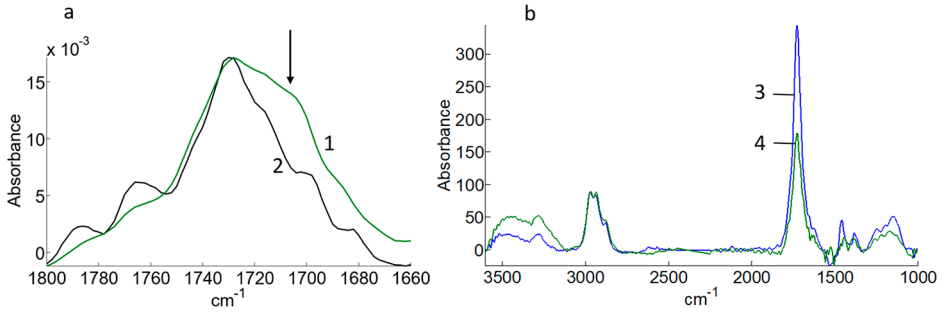

Figure 10. (a) Comparison of the mean IR spectra between the hydrophilic mix area (1) and the PMA hydrophobic area (2) taken in the regions shown in Figure 9a. The wavenumber range corresponds to that of the C═O stretching band. (b) Comparison of the mean IR spectra between the hydrophobic PMA area (3) and the hydrophilic O_2-plasma treated PMA area (4) taken in the regions shown in Figure 9b. The spectra are normalized to the CH_2/CH_3 stretching band (2900−2600 cm^{-1}).

DOI: 10.1021/acs.langmuir.9b00493
Langmuir 2019, 35, 9677−9683

interface, and that local chemical heterogeneity can be easily achieved with the masking and sequential plasma deposition methodology developed herein.

In the case of the Mix on PMA sample, the main difference is a shoulder appearing on the C═O stretching band in the hydrophilic area (arrow, Figure 10a). Indeed, the Mix area contains acrylic acid, and this shoulder can be associated with the presence of carboxylic acid groups in the film. For the PMA on O_2-treated PMA sample, the chemical difference between the areas is reflected by the higher intensity of the OH stretching band in the mean spectrum of the hydrophilic area (Figure 10b).

CONCLUSION

A simple, robust, and tunable method to synthesize hybrid patterned and laminate hydrophilic/phobic coatings with submm spatial resolution was developed. The method utilizes an atmospheric pressure dielectric barrier discharge with PMA and AA precursors and shadow masks. Despite the apparent similarity in chemical structure of the precursors, the deposited coatings exhibited WCA varying from <5° to >125°, depending on the deposition parameters, demonstrating the power, ease, and tunability of atmospheric pressure plasma-based film deposition. The double and triple bonds located at both ends of PMA ensure not only a high deposition rate but also cross-linking that favors the formation of a stable, water insoluble layer. The originality and utility of the combined precursor method ensures perfect miscibility, with adjustable polar vs carboxylic acid functionalities that allows precise tuning of surface wettability.

AUTHOR INFORMATION

Corresponding Author

*E-mail: ademaude@ulb.ac.be.

ORCID

A. Demaude: 0000-0003-1387-8691
R. Lazzaroni: 0000-0002-6334-4068
A. Delcorte: 0000-0003-4127-8650
M. Gordon: 0000-0003-0123-9649
F. Reniers: 0000-0001-9331-6060

Notes

The authors declare no competing financial interest.

ACKNOWLEDGMENTS

This work was partly funded by the Hylife, Flycoat and SmartHycar projects (Walloon Region, and M-EraNet, Belgium).

REFERENCES

(1) Zhang, S.; Huang, J.; Chen, Z.; Lai, Y. Bioinspired Special Wettability Surfaces: From Fundamental Research to Water Harvesting Applications. *Small* **2017**, *13* (3), 1602992

(2) Ueda, E.; Levkin, P. A. Emerging Applications of Superhydrophilic-Superhydrophobic Micropatterns. *Adv. Mater.* **2013**, *25* (9), 1234−1247.

(3) Liu, X.; Wang, Q.; Qin, J.; Lin, B. A Facile "Liquid-Molding" Method to Fabricate PDMS Microdevices with 3-Dimensional Channel Topography. *Lab Chip* **2009**, *9* (9), 1200−1205.

(4) Leclair, A. M.; Ferguson, S. S. G.; Lagugné-Labarthet, F. Surface Patterning Using Plasma-Deposited Fluorocarbon Thin Films for Single-Cell Positioning and Neural Circuit Arrangement. *Biomaterials* **2011**, *32* (5), 1351−1360.

(5) Tsougeni, K.; Bourkoula, A.; Petrou, P.; Tserepi, A.; Kakabakos, S. E.; Gogolides, E. Photolithography and Plasma Processing of Polymeric Lab on Chip for Wetting and Fouling Control and Cell Patterning. *Microelectron. Eng.* **2014**, *124*, 47−52.

(6) Ganesh, V. A.; Raut, H. K.; Nair, A. S.; Ramakrishna, S. A Review on Self-Cleaning Coatings. *J. Mater. Chem.* **2011**, *21* (41), 16304−16322.

(7) Parker, A. R.; Lawrence, C. R. Water Capture by a Desert Beetle. *Nature* **2001**, *414* (6859), 33−34.

(8) Xu, G.; Liu, P.; Pranantyo, D.; Neoh, K.-G.; Kang, E.-T. Dextran and Chitosan-Based Antifouling, Antimicrobial Adhesion and Self-Polishing Multilayer Coatings from pH-Responsive Linkages-Enabled Layer-by-Layer Assembly. *ACS Sustain. Chem. Eng.* **2018**, *6*, 3916.

(9) Nishimoto, S.; Becchaku, M.; Kameshima, Y.; Shirosaki, Y.; Hayakawa, S.; Osaka, A.; Miyake, M. TiO_2-Based Superhydrophobic - Superhydrophilic Pattern with an Extremely High Wettability Contrast. *Thin Solid Films* **2014**, *558*, 221−226.

(10) Ren, D.; Xia, Y.; Wang, J.; You, Z. Micropatterning of Single Cell Arrays Using the PEG-Silane and Biotin−(Strept)Avidin System with Photolithography and Chemical Vapor Deposition. *Sens. Actuators, B* **2013**, *188*, 340−346.

(11) Liimatainen, V.; Shah, A.; Johansson, L.-S.; Houbenov, N.; Zhou, Q. Maskless, High-Precision, Persistent, and Extreme Wetting-Contrast Patterning in an Environmental Scanning Electron Microscope. *Small* **2016**, *12* (14), 1847−1853.

(12) Graz, I.; Ebner, A.; Bauer, S.; Romanin, C.; Gruber, H. Micropatterned Atmospheric Pressure Discharge Surface Modification of Fluorinated Polymer Films for Mammalian Cell Adhesion and Protein Binding. *Appl. Phys. A: Mater. Sci. Process.* **2008**, *92* (3), 547−555.

(13) Nørgaard, T.; Dacke, M. Fog-Basking Behaviour and Water Collection Efficiency in Namib Desert Darkling Beetles. *Front. Zool.* **2010**, *7* (1), 23.

(14) Cools, P.; Declercq, H.; De Geyter, N.; Morent, R. A Stability Study of Plasma Polymerized Acrylic Acid Films. *Appl. Surf. Sci.* **2018**, *432*, 214−223.

(15) Ben Salem, D.; Carton, O.; Fakhouri, H.; Pulpytel, J.; Arefi-Khonsari, F. Deposition of Water Stable Plasma Polymerized Acrylic Acid/MBA Organic Coatings by Atmospheric Pressure Air Plasma Jet: Deposition of Water Stable Plasma Polymerized AA/MBA. *Plasma Processes Polym.* **2014**, *11* (3), 269−278.

(16) Kong, Y.; Lin, X.; Wu, Y.; Chen, J.; Xu, J. Plasma Polymerization of Octafluorocyclobutane and Hydrophobic Microporous Composite Membranes for Membrane Distillation. *J. Appl. Polym. Sci.* **1992**, *46* (2), 191−199.

(17) Nisol, B.; Ghesquière, J.; Reniers, F. Easy Synthesis of Ageing-Resistant Coatings with Tunable Wettability by Atmospheric Pressure Plasma. *Plasma Chem. Plasma Process.* **2016**, *36* (5), 1239−1252.

(18) Nisol, B.; Arnoult, G.; Bieber, T.; Kakaroglou, A.; De Graeve, I.; Van Assche, G.; Terryn, H.; Reniers, F. About the Influence of Double Bonds in the APPECVD of Acrylate-Like Precursors: A Mass Spectrometry Study of the Plasma Phase. *Plasma Process. Polym.* **2014**, *11* (4), 335−344.

(19) Naderi-Gohar, S.; Huang, K. M. H.; Wu, Y.; Lau, W. M.; Nie, H.-Y. Depth Profiling Cross-Linked Poly(Methyl Methacrylate) Films: A Time-of-Flight Secondary Ion Mass Spectrometry Approach: Depth Profiling Cross-Linked PMMA Films: A TOF-SIMS Approach. *Rapid Commun. Mass Spectrom.* **2017**, *31* (4), 381−388.

(20) Nie, H.-Y. Negative Hydrocarbon Species $C_{2n}H^-$: How Useful Can They Be? *J. Vac. Sci. Technol., B: Nanotechnol. Microelectron.: Mater., Process., Meas., Phenom.* **2016**, *34* (3), 030603.

(21) Alexer, M. R.; Duc, T. M. The Chemistry of Deposits Formed from Acrylic Acid Plasmas. *J. Mater. Chem.* **1998**, *8* (4), 937−943.

DOI: 10.1021/acs.langmuir.9b00493
Langmuir 2019, 35, 9677−9683